Proc. Natl. Acad. Sci. USA
Vol. 86, pp. 2985–2989, April 1989
Psychology

Two motion perception mechanisms revealed through distance-driven reversal of apparent motion

CHARLES CHUBB AND GEORGE SPERLING

Human Information Processing Laboratory, Department of Psychology, New York University, 6 Washington Place, New York, NY 10003

Contributed by George Sperling, December 30, 1988

ABSTRACT **We demonstrate two kinds of visual stimuli that exhibit motion in one direction when viewed from near and in the opposite direction from afar. These striking reversals occur because each kind of stimulus is constructed to simultaneously activate two different mechanisms: a short-range mechanism that computes motion from space–time correspondences in stimulus luminance and a long-range mechanism in which motion computations are performed, instead, on stimulus contrast that has been full-wave rectified (e.g., on the absolute value of contrast).**

We demonstrate two dynamic visual stimuli that appear to move in one direction when viewed from near and in the opposite direction from afar. This remarkable reversal of apparent motion occurs because the stimuli are constructed to simultaneously activate two different mechanisms: a first-order mechanism that computes motion from space–time correspondences in raw stimulus *luminance* and a second-order mechanism that uses, instead, a *full-wave* rectified transformation (e.g., the absolute value) of stimulus *contrast* to compute motion.

The first stimulus, B, a rightward stepping, contrast-reversing bar, is a variant of Anstis's (1) reversed-phi stimulus. What we add are quite different explanations of the ordinary and the reversed motions in this stimulus and the conditions under which each is perceived.

The second stimulus, Γ, a stepping, contrast-reversing grating, is an elaboration of the first with two useful properties: (*i*) It provides the first- and second-order systems with motion signals of identical spatial frequency, moving at the same rate, but in opposite directions; and (*ii*) its motion direction is totally ambiguous to any half-wave rectifying system. The dominance of the first-order mechanism when the retinal image is small (far-viewing) suggests that it is the mechanism of Braddick's (2) short-range system; the dominance of the second-order mechanism with large retinal images suggests that it is the mechanism of the long-range system.

Since Braddick (2) proposed that there are two motion perception mechanisms with different properties—a short-range and long-range motion-perception system, the issue has been intensely investigated (3–16). The following differences between the short-range and long-range systems are proposed. The short-range system requires successive stimuli to be displaced in space by a small distance Δx within a small time period Δt and presented to the same eye. The long-range system tolerates large Δx, Δt, and interocular presentation (2, 12).

Anstis and Mather (16) noted that in making its matches across time and space, the long-range system is indifferent to sign of contrast: Motion is generated between successively displayed, spatiotemporally displaced points on a grey background, even when they are of opposite contrast polarity (i.e., one is white and the other black). Quite the reverse is true of the short-range system. The sensitivity of the short-range system to the sign of contrast is exhibited strikingly in the phenomenon of *reversed*-phi apparent motion (1): When a picture is flashed twice in quick succession, with the second flash slightly displaced in space from the first, motion (called ϕ motion) is perceived in the direction of the displacement. However, if the contrast of the picture is reversed between the first and second flash, motion may be perceived in the direction *opposite* to the displacement. This is *reversed*-phi motion.

What has been lacking is a clear specification of the mechanisms governing the short- and long-range systems. Here we introduce two stimuli, the contrast reversing bar B (Fig. 1*d*) and the stepping, contrast-reversing grating Γ (see Fig. 2*a*) that display short-range (reversed-phi) motion to the left when viewed from far away and long-range motion to the right when viewed from a short distance. Γ is constructed so as to place important constraints on the underlying mechanisms that detect the motion it displays from both far and near viewing distances. Specifically, Γ rules out the possibility that either sort of motion is mediated by *half-wave* rectification. Rather, Γ strongly suggests that the short-range system applies what we shall call standard motion analysis to raw stimulus *luminance*, while the particular long-range system stimulated by Γ from short viewing distances applies standard motion analysis to a *full-wave* rectified transformation of stimulus *contrast*.

A monochromatic visual stimulus is a function that assigns a luminous flux to each point in space–time. However, from a perceptual point of view, a stimulus is better described by its contrast than by its luminance l. Thus, a stimulus S is the normalized deviation of $l(x, y, t)$ from its mean luminance l_0; that is, for any point x, y, t in space–time, $S(x, y, t) = [l(x, y, t) - l_0]/l_0$. Because a stimulus is defined in terms of the contrast-modulation function S (rather than the raw luminance function l), stimulus values (unlike luminance values) may be positive or negative.

To simplify the discussion, we consider only stimuli that do not vary in the vertical dimension, i.e., stimuli that can be described as horizontally moving patterns of vertically oriented bars. Any such vertically-constant stimulus is characterized in all relevant respects by its xt cross-section $S(x, t)$, a slice made perpendicular to the vertical axis of space to reveal stimulus contrast as a function of horizontal space (x) and time (t).

Fig. 1*a* depicts eight frames of a movie of a dark vertical bar stepping left-to-right across a bright field. Fig. 1*b* is the xt cross-section of the rightward-stepping dark bar. Fig. 1*c* shows an xt cross-section of a rightward-drifting, vertically oriented sine-wave grating $S(x, t) = \sin(x - t)$. This sine-wave component of *b* is shown superimposed on *b*. Fig. 1*c* illustrates how the detection of motion in a complex stimulus can be understood in terms of motion of the sine-wave components.

It is immediately obvious from the xt cross-sections of the rightward-stepping bar and sine-wave stimuli that the prob-

The publication costs of this article were defrayed in part by page charge payment. This article must therefore be hereby marked "*advertisement*" in accordance with 18 U.S.C. §1734 solely to indicate this fact.

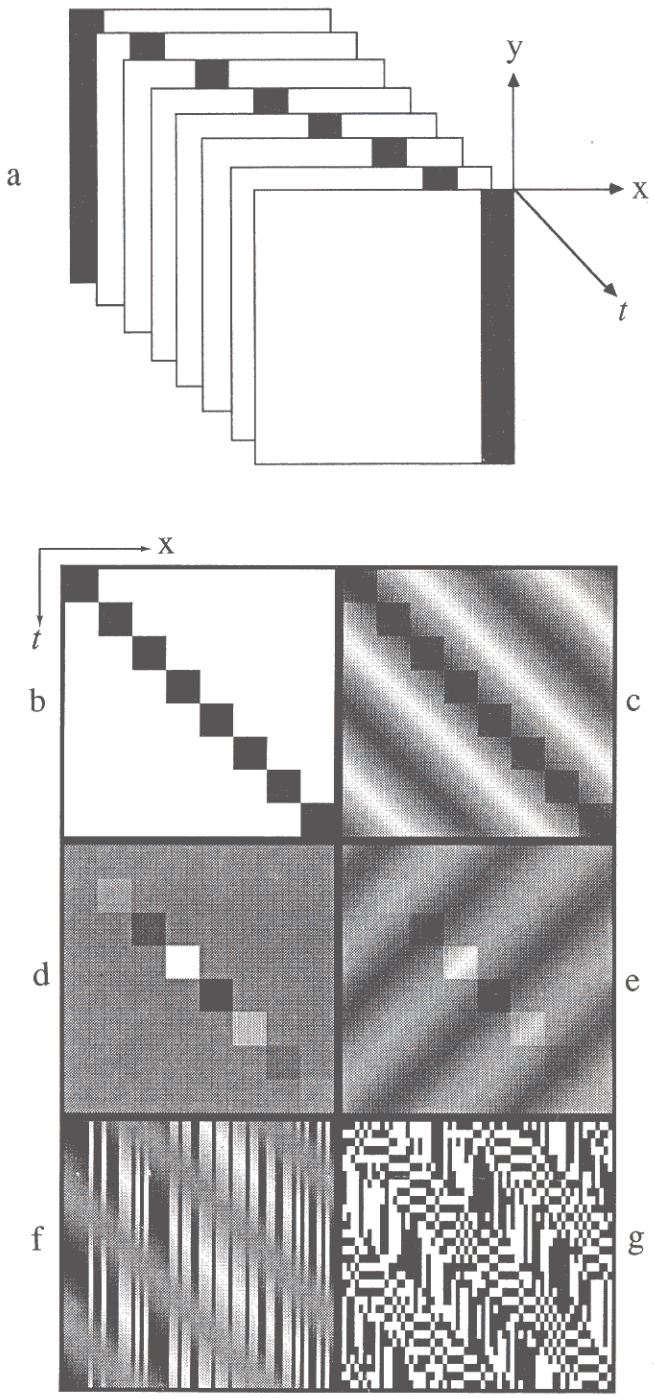

FIG. 1. Slant in x and y corresponds to motion in xt. (*a*) Eight frames in a display of a rightward-stepping, vertical bar; x and y represent the spatial dimensions of the display, and t represents time. This stimulus does not vary in the y dimension. Each of panels *b*–*g* is an xt cross-section of a dynamic stimulus that does not vary in y. (*b*) An xt cross-section of the rightward-stepping bar of panel *a*. Horizontal luminances are indicated along x; temporal luminances are indicated vertically with time t running downward. (*c*) Stimulus of *b* shown together with one of its largest sinusoidal components. (*d*) The Gaussian windowed, contrast-reversing stepping bar—stimulus B. (*e*) Stimulus B shown together with its largest sinusoidal component, indicating why its far view (first-order, Fourier) motion is to the left. (*f*) A row of vertical bars, randomly of positive or negative contrast, the amplitude of which is modulated by a rightward-drifting grating; (*g*) a row of random, black/white vertical bars the flicker rate of which is modulated by a rightward-drifting grating. The motion of all four stimuli is as obvious to all viewers as is the slant of the x, t cross-section. The rightward motion of the black bar (*b* and *c*), and the leftward far-view motion of the contrast-reversing bar B (*d* and *e*) are accessible to first-order mechanisms; the rightward motion of stimuli (*f* and *g*), and the rightward near-view motion of B (*d*) are not. The motion of stimulus *f* can be exposed to standard analysis by simple half- or full-wave rectification; stimulus *g* requires a temporal linear filter (e.g., a temporal differentiator) before rectification.

lem of detecting motion in xt is equivalent to the problem of detecting orientation in xy. That is, the perception of an xy pattern slanting down to the right is analogous to the perception of an xt pattern moving to the right.

Fig. 1*d* shows the contrast-reversing bar B, which is Gaussian-windowed in time. When the bar takes 60 steps per sec (one step every 17 msec) and is windowed by a Gaussian function with SD of 25 msec, every observer so far has reported the direction of motion as being to the right when viewed in central vision from a wide range of near distances. On the other hand, B appears to be moving leftward when viewed in peripheral vision from near or when viewed in central vision from afar over a smaller range of distances near the vanishing point. Fig. 1*e* suggests the Fourier basis of the far-view motion; the dominant sine-wave components are leftward (17). We momentarily defer the explanation of rightward movement.

Visual slant detection (often called orientation detection) is generally thought to involve oriented Hubel–Wiesel (18) receptive fields in area 17 of the visual cortex. The corresponding computational mechanisms are oriented linear filters (19, 20). The detection of slant, however, involves a further (inherently nonlinear) stage of processing: A decision about the dominant slant of a spatial stimulus S must be made with reference to the relative energy in the responses-to-S of various linear filters in different phases and orientations. A wide range of models to explain slant (and motion) perception apply computations of this sort to the visual stimulus (17, 21–28), and similar computations are coming to have wide applications in robotic vision (29, 30).

Although exclusively spatial detectors are physically different from spatiotemporal detectors, the computations for orientation-detection and motion-detection are quite similar. For both slant and motion, the quantity computed by any energy-analytic detector can be cast as a linear combination of the pairwise products of stimulus values, $S(x_i, t_i)S(x_j, t_j)$, for i and j both ranging over all points in space–time. (For slant detectors the time variables t_i and t_j are replaced by vertical space variables y_i and y_j.) We refer to computations of this sort as *standard motion* (or *slant*) *analysis*.

Let D_1 be a standard motion analyzer defined for any stimulus S by

$$D_1(S) = \sum_i \sum_j W_{i,j} S(x_i, t_i) S(x_j, t_j), \qquad [1]$$

where each $W_{i,j}$ is a real-valued weight. The standard motion analyzer tuned to the same sort of motion as D_1, but in the opposite direction, is

$$D_2(S) = \sum_i \sum_j W_{i,j} S(x_i, t_j) S(x_j, t_i). \qquad [2]$$

Any stimulus S is called microbalanced if and only if for any such oppositely tuned standard motion analyzers, D_1 and D_2, the expected response $E[D_1(S)]$ is equal to the expected response $E[D_2(S)]$ (31).

Although, as this definition indicates, microbalanced random stimuli yield no signs of systematic motion to standard motion analysis, it is nonetheless possible to construct a wide variety of microbalanced random stimuli that display consistent motion across independent realizations (31, 32). For example, the amplitude-modulated noise stimulus I and the frequency-modulated noise stimulus J in Fig. 1*f* and *g* (31) are microbalanced. Nonetheless, observers universally perceive

the dynamic versions of these stimuli as moving rightward, and the texture versions as slanted downward to the right.

Following Cavanagh†, we call any motion mechanism that applies standard motion (or slant) analysis directly to luminance (or to a linear transformation of luminance) a first-order mechanism. Any motion mechanism that applies standard motion (or slant) analysis to a grossly nonlinear transformation of luminance is called a second-order mechanism.

There is a simple way to expose the inherent motion (or slant) in stimuli such as *I* and *J*: (*i*) apply a temporal (or vertical) linear filter, (*ii*) rectify the result, and (*iii*) apply standard analysis.‡ There are two candidate schemes of rectification: full-wave rectification, which consists of computing the absolute value (or a monotonically increasing function of the absolute value) of the filtered contrast, and half-wave rectification, which consists of making independent, separate computations on positive and on negative values of filtered contrast. Full-wave rectification has a long history of utility in signal processing. Half-wave rectification appears to be a widespread, almost universal, physiological process: Because neurons have only a positive output (their firing frequency), they are paired in order to economically convey positive and negative signal values. In the visual system, one pair-member (an "on-center" neuron) carries values of positive contrast, whereas its pair-mate (an "off-center" neuron) carries negative contrast values.

The phenomenon of reversed-phi motion (1) demonstrated in the far viewing of Fig. 1*d* [and many similar results (17)] could not occur if the short-range system applied a full-wave rectifier before standard motion analysis. Simple full-wave rectification of contrast obliterates the difference between the simple moving bar (Fig. 1*b*) and corresponding contrast-reversing bar (B, Fig. 1*d*). Any mechanism that full-wave rectified contrast before motion analysis would issue similar responses for the stimuli of Fig. 1 *b* and *d*.

These considerations do not, however, rule out the possibility that the short-range system uses a half-wave rectifier before standard motion analysis (33). Perhaps both short-range motion and the motion of various microbalanced random stimuli such as *I* (Fig. 1*f*) and *J* (Fig. 1*g*) can be explained with reference to a single kind of mechanism; one that applies to stimulus contrast a linear filter, then a half-wave rectifier, and finally some form of standard motion analysis. Or perhaps, as seems more likely, short-range motion results from applying standard motion analysis directly to contrast. In this case, we are left with the question of what sorts of rectification are involved in perceiving the motion of microbalanced random stimuli.

These issues are cleared up by the leftward-stepping, contrast-reversing grating Γ defined in Fig. 2. An *xt* cross-section of Γ is shown in Fig. 2*a*. The temporal scale and the (distance-dependent) spatial scale of the display are described in the legend for Fig. 2. Γ is perceived to move leftward from near viewing distances and rightward from far distances. Γ has been viewed by dozens of subjects in our lab, and the reversal of apparent motion with viewing distance has been observed by all.

The far-view motion of Γ is detected by the short-range system. Note that in each successive display, Γ is shifted 1/4 spatial cycle leftward, and its contrast is reversed. Thus, we should expect Γ to elicit reversed-phi motion under appropriate conditions. And indeed, when the spatial displacement between successive displays is made sufficiently small by moving the viewer back from the screen, Γ exhibits reversed-phi motion to the right, implicating the short-range system. The velocity of this far-view motion is easily distinguished by all subjects and is equal to that of the grating overlaid on Γ in Fig. 2*b*. As this overlay makes clear, the far-view motion of Γ is signaled directly by the distribution of energy in the Fourier transform of Γ. Typically, standard motion-analytic computations reflect this distribution of Fourier energy in the stimulus. Thus, the far-view motion of Γ is the predicted response of a first-order mechanism.

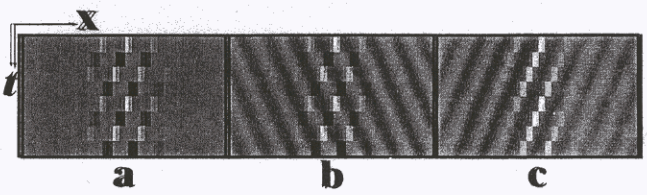

FIG. 2. Graphic analysis of the motion content of stimulus Γ, a horizontally windowed, leftward-stepping grating of vertical bars that reverses contrast with each step. (*a*) An *xt* cross-section of Γ. Γ is temporally periodic. The temporal slice displayed here contains eight frames, each of which lasts 1/15 sec; thus, the total duration shown is 533 msec. From far (8 m), the width of *a* is ≈0.6 degrees of visual angle (dva), and each vertical bar in the grating has a width of 0.02 dva. (*b*) A sinusoid is overlaid on Γ to illustrate the perceived motion of Γ when viewed from 8 m. Conformity to sinusoidal analysis suggests that the far-view motion of Γ is first-order. (*c*) |Γ|, the absolute value (full-wave rectified) transformation of Γ. From near (2 m), the stimulus Γ displays motion conforming to the sinusoid overlaid on |Γ|, suggesting that the near-view motion of Γ is second-order and possibly mediated by full-wave rectification of stimulus contrast.

By contrast, the near-view motion of Γ is detected by a second-order mechanism. It is evident to all viewers that the leftward motion displayed by Γ from short viewing distances is carried directly by the leftward-stepping, contrast-reversing, vertical bars. However, Γ has no energy in any Fourier component (drifting sinusoidal grating) whose velocity matches that of these leftward-stepping bars. This indicates that the near-view motion of Γ is not obtained directly by standard analysis. We can, however, expose the near-view motion of Γ by full-wave rectifying Γ before standard motion analysis. This is illustrated by Fig. 2*c*, in which |Γ| is shown, overlaid by a leftward-drifting grating that contributes strongly to it. The velocity of this sinusoid is precisely the velocity of the near-view motion of Γ.

There are other transformations aside from simple full-wave rectification that might expose the near-view motion of Γ to standard analysis. The most likely transformations (31, 32, 34) involve an initial stage of temporal linear filtering. Plausible candidates are filters whose response at every point (x,y) in space depends on (*i*) average recent stimulus contrast at that point and/or (*ii*) recent changes in contrast at that point. In particular, the likely temporal filters are marked by brief impulse responses (most of their energy confined to <100 msec) that (*i*) integrate to a nonzero value (so as to reflect raw stimulus contrast) and/or (*ii*) are biphasic (so as to register quick changes in contrast). Some candidate impulse responses are plotted in Fig. 3, *a*–*c*.

What distinguishes the leftward-stepping, contrast-reversing grating Γ from other stimuli that reverse direction of motion with viewing distance (34) is that, for all of these empirically plausible temporal linear filters $f*$ (e.g., with impulse response f conforming to Fig. 3 *a*, *b*, or *c*), the result of half-wave rectifying $f * \Gamma$ is completely ambiguous in motion content.

Half-wave ambiguity of Γ and its transformations is illustrated in Fig. 3. The filter $g*$, whose impulse response g is shown in Fig. 3*a*, is a physiologically plausible representation of the identity transformation; $g*$ averages recent contrast but does not register sudden changes in contrast. The filter $k*$, whose impulse response k is shown in Fig. 3*c*, is a

†Cavanagh, P., Conference on Visual Form and Motion Perception: Psychophysics, Computation, and Neural Networks, March 5, 1988, Boston University, Boston, MA.

‡Rectification alone suffices to expose the motion of *I* to standard analysis; temporal differentiation and rectification are required for *J*.

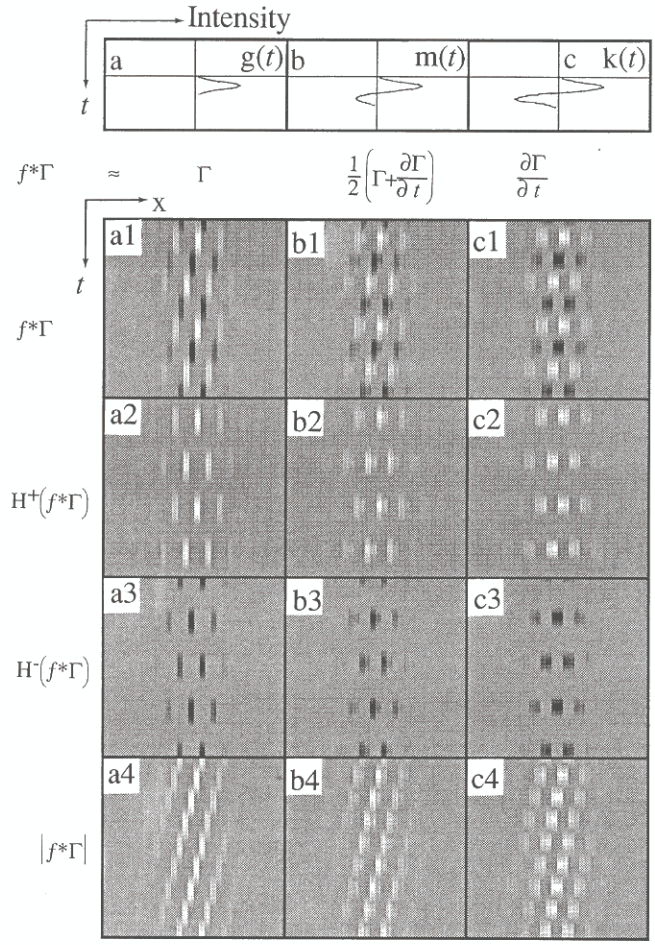

FIG. 3. Exposing the near-view motion of Γ to standard analysis. The vertical dimension in all panels is time t, running downward. The scale of t is constant throughout the figure (see below). Each panel in the first row represents the impulse response f of a temporal filter that is an empirically plausible initial stage of a rectifying, second-order motion mechanism. The horizontal axis of each panel in the first row indicates intensity, increasing left-to-right. (*a*) Impulse response of a physiologically plausible approximation to the temporal identity: it averages recent stimulus contrast. (*c*) A physiologically plausible approximation to a temporal differentiator: it responds only to temporal changes in contrast. (*b*) The average of responses of filters *a* and *c*, a physiologically plausible compromise between temporal differentiator and identity that indicates both recent changes in contrast and recent average contrast. The panels (*a1–c4*) are *xt* cross-sections; the horizontal axes indicate horizontal space, the vertical axes indicate time. Each grey panel spans 2.4° of visual angle horizontally at a viewing distance of 2 m and spans 533 msec (vertically). In the row $f * \Gamma$ and the column under each impulse response is a *xt* cross-section of the result of applying filter f to Γ (Fig. 2*a*). Subsequent rows indicate the result of rectifying $f * \Gamma$. $H^+(f * \Gamma)$ and $H^-(f * \Gamma)$ indicate the positive and negative half-wave components of the same-column linear transformation, and the row marked $|f * \Gamma|$ shows full-wave rectifications of these temporal filterings of Γ. All half-wave components are ambiguous in motion content; all full-wave rectifications yield unambiguous leftward motion to standard analysis.

physiologically plausible approximation to a temporal differentiator ($k*$ registers temporal changes in contrast, without keeping track of average recent contrast). The best-of-both-worlds filter $m*$ has impulse response $m = (g + k)/2$ shown in Fig. 3*b*. The reason for including this best-of-both-worlds filter is that among the stimuli that display second-order motion mediated by temporal filtering, there are some for which $g*$ (Fig. 3*a*) works but not $k*$ (Fig. 3*c*), and some for which $k*$ (Fig. 3*c*) works but not $g*$ (Fig. 3*a*); however, $m*$ (Fig. 3*b*) works for all (32).

In Fig. 3, the top row of *xt* cross-sections (marked $f * \Gamma$) displays the result of applying each of the filters directly to Γ. The rows marked $H^+(f * \Gamma)$ (Fig. 3 *a2, b2*, and *c2*) and $H^-(f * \Gamma)$ (Fig. 3 *a3, b3*, and *c3*) display the positive and negative half-wave components of the same-column, filtered outputs (Fig. 3 *a1, b1*, and *c1*), and the row marked $|f * \Gamma|$ displays full-wave rectifications (Fig. 3 *a4, b4*, and *c4*) of the filter outputs. The important fact graphically illustrated here is that the half-wave components of all of these linear transformations of Γ are completely ambiguous in motion content. As Fig. 3 *a4, b4*, and *c4* make clear, full-wave rectification works to expose the near-view motion of Γ; however, almost any full-wave-like rectification that combines same-sign output for positive and negative signal components will also work.

The distance-driven reversal of the apparent motion displayed by the leftward-stepping, contrast-reversing grating Γ (Fig. 2*a*) makes it dramatically clear that, as many have observed (2, 16, 30–38), the visual system extracts motion information from the visual signal in more than one way. Fig. 2 *b* and *c* illustrate that the far-view motion of Γ is consonant with a first-order mechanism (i.e., a Fourier mechanism that applies some form of standard motion analysis directly to the untransformed stimulus), whereas the near-view motion of Γ implicates a second-order mechanism that applies standard motion analysis to a rectified transformation of Γ (e.g., |Γ|, Fig. 2*c*). In the context of the various stimuli we have been able to create, the motion of which reverses with distance (33), the specific importance of Γ derives from the fact that the near-view motion of Γ cannot be exposed to standard motion analysis by any of the empirically plausible linear filters followed by half-wave rectification, whereas full-wave rectification works in conjunction with all the plausible filters.

It is possible to construct stimuli the motion of which is accessible neither to first-order mechanisms nor to any of the second-order mechanisms considered here (32). The question remains open as to whether any of the mechanisms that detect these other sorts of motion use half-wave rectification. However, the leftward-stepping, contrast-reversing grating Γ conclusively establishes that at least one second-order mechanism uses full-wave rectification.

This work was supported by Air Force Office of Scientific Research, Life Sciences Directorate, Vision Information Processing Program, Grants 85-0364 and 88-0140.

1. Anstis, S. M. (1970) *Vision Res.* **10,** 1411–1430.
2. Braddick, O. (1974) *Vision Res.* **14,** 519–527.
3. Lappin, J. S. & Bell, H. H. (1976) *Vision Res.* **16,** 161–168.
4. Westheimer, G. & McKee, S. P. (1977) *Vision Res.* **17,** 887–892.
5. Bell, H. H. & Lappin, J. S. (1979) *Percept. Psychophys.* **26,** 415–417.
6. Baker, C. L. & Braddick, O. (1982) *Vision Res.* **22,** 851–856.
7. Baker, C. L. & Braddick, O. (1982) *Vision Res.* **22,** 1253–1260.
8. Chang, J. J. & Julesz, B. (1983) *Vision Res.* **23,** 639–646.
9. Chang, J. J. & Julesz, B. (1983) *Vision Res.* **23,** 1379–1386.
10. Chang, J. J. & Julesz, B. (1985) *Spatial Vision* **1,** 39–45.
11. Ramachandran, V. S. & Anstis, S. M. (1983) *Vision Res.* **23,** 1719–1724.
12. Westheimer, G. (1983) *Vision Res.* **23,** 759–763.
13. Bennett, R. G. & Westheimer, G. (1985) *Vision Res.* **25,** 565–569.
14. Nakayama, K. & Silverman, G. (1984) *Vision Res.* **24,** 293–300.
15. van Doorn, A. J. & Koenderink, J. J. (1984) *Vision Res.* **24,** 47–54.
16. Anstis, S. M. & Mather, G. (1985) *Perception* **14,** 167–179.
17. van Santen, J. P. H. & Sperling, G. (1984) *Opt. Soc. Am. A* **1,** 451–473.
18. Hubel, D. H. & Wiesel, T. N. (1959) *J. Physiol. (London)* **148,** 574–591.
19. Granlund, G. H. & Knutsson, H. (1983) in *Physical and Biological Processing of Images*, eds. Braddick, O. J. & Sleigh, A. C. (Springer, New York), pp. 282–303.

20. Watson, A. B. (1983) in *Physical and Biological Processing of Images*, eds. Braddick, O. J. & Sleigh, A. C. (Springer, New York), pp. 100–114.
21. Reichardt, W. (1957) *Z. Naturforschung* **12**, 447–457.
22. Adelson, E. H. & Bergen, J. (1985) *J. Opt. Soc. Am. A* **2**, 284–299.
23. Watson, A. B. & Ahumada, A. J. (1983) *A Look at Motion in the Frequency Domain* NASA Technical Memorandum 84352 (Natl. Aeronautics and Space Admin., Ames Research Center, CA).
24. Watson, A. B. & Ahumada, A. J. (1985) *J. Opt. Soc. Am. A* **2**, 322–342.
25. van Santen, J. P. H. & Sperling, G. (1985) *J. Opt. Soc. Am. A* **2**, 300–321.
26. Fleet, D. J. & Jepson, A. D. (1985) *On the Hierarchical Construction of Orientation and Velocity Selective Filters*, Technical Report RBCV-TR-85-8. (Univ. Toronto Comp. Sci. Dept., Toronto, ON).
27. Heeger, D. J. (1987) *J. Opt. Soc. Am A* **4**, 1455–1471.
28. Reichardt, W. & Egelhaaf, M. (1988) *Z. Naturwissenschaften* **75**, 313–315.
29. Anandan, P. (1988) in *Proceedings of the First International Conference on Computer Vision* (IEEE Comp. Soc., Washington, DC), pp. 219–230.
30. Waxman, A. M. & Bergholm, F. (1987) *Convected Activation Profiles and Image Flow Extraction*, Laboratory for Sensory Robotics Technical Report 4, (Boston Univ., Boston, MA).
31. Chubb, C. & Sperling, G. (1988) *J. Opt. Soc. Am. A* **5**, 1986–2007.
32. Chubb, C. & Sperling, G. (1989) *Proceedings: 1989 IEEE Workshop on Motion.* (IEEE Computer Society, Washington, DC).
33. Walt, R. J. & Morgan, M. J. (1985) *Vision Res.* **25**, 1661–1674.
34. Chubb, C. & Sperling, G. (1988) *Invest. Ophthalmol. Vis. Sci.* **29**, 266.
35. Chubb, C. & Sperling, G. (1988) *Mathematical Studies in Perception and Cognition*, 88-1 (New York Univ., New York).
36. Chubb, C. & Sperling, G. (1987) *Invest. Ophthalmol. Vis. Sci.* **28**, 233.
37. Pantle, A. & Picciano, L. (1976) *Science* **193**, 500–502.
38. Lelkens, A. M. M. & Koenderink, J. J. (1984) *Vision Res.* **24**, 1083–1090.